



Restoration of coronary microvascular function by OGA overexpression in a high-fat diet with low-dose streptozotocin-induced type 2 diabetic mice

Diabetes & Vascular Disease Research
 May-June 2023: 1–13
 © The Author(s) 2023
 Article reuse guidelines:
sagepub.com/journals-permissions
 DOI: 10.1177/14791641231173630
journals.sagepub.com/home/dvr


Jody Tori Cabrera^{1,**}, Rui Si^{2,3,**}, Atsumi Tsuji-Hosokawa^{2,**}, Hua Cai⁴, Jason X-J Yuan¹, Wolfgang H Dillmann¹ and Ayako Makino^{1,2} 

Abstract

Sustained hyperglycemia results in excess protein O-GlcNAcylation, leading to vascular complications in diabetes. This study aims to investigate the role of O-GlcNAcylation in the progression of coronary microvascular disease (CMD) in inducible type 2 diabetic (T2D) mice generated by a high-fat diet with a single injection of low-dose streptozotocin. Inducible T2D mice exhibited an increase in protein O-GlcNAcylation in cardiac endothelial cells (CECs) and decreases in coronary flow velocity reserve (CFVR, an indicator of coronary microvascular function) and capillary density accompanied by increased endothelial apoptosis in the heart. Endothelial-specific O-GlcNAcase (OGA) overexpression significantly lowered protein O-GlcNAcylation in CECs, increased CFVR and capillary density, and decreased endothelial apoptosis in T2D mice. OGA overexpression also improved cardiac contractility in T2D mice. OGA gene transduction augmented angiogenic capacity in high-glucose treated CECs. PCR array analysis revealed that seven out of 92 genes show significant differences among control, T2D, and T2D + OGA mice, and *Sp1* might be a great target for future study, the level of which was significantly increased by OGA in T2D mice. Our data suggest that reducing protein O-GlcNAcylation in CECs has a beneficial effect on coronary microvascular function, and OGA is a promising therapeutic target for CMD in diabetic patients.

Keywords

Diabetes, cardiovascular disease, endothelial dysfunction, angiogenesis, tube formation

Introduction

Diabetes-induced cardiovascular complications have become one of the major health concerns as the global trend of diabetes prevalence continues to grow. Heart-related vascular complications in diabetic patients include obstructive coronary artery disease (CAD)¹ and coronary microvascular disease (CMD).² Obstructive CAD is known to be a primary cause of cardiac ischemia; however, there is rising evidence showing that CMD, also known as non-obstructive CAD, is an additional cause for increased cardiac mortality.^{3–5} Coronary endothelial dysfunction is

¹Department of Medicine, University of California, San Diego, La Jolla, CA, USA

²Department of Physiology, The University of Arizona, Tucson, AZ, USA

³Department of Cardiology, Xijing Hospital, Fourth Military Medical University, Shaanxi, China

⁴Department of Anesthesiology, University of California, Los Angeles, Los Angeles, CA, USA

**Equal contribution.

Corresponding author:

Ayako Makino, Division of Endocrinology and Metabolism, Department of Medicine, University of California, San Diego, 9500 Gilman Drive, MC-0856, La Jolla, CA 92093, USA.

Email: amakino@health.ucsd.edu



Creative Commons Non Commercial CC BY-NC: This article is distributed under the terms of the Creative Commons Attribution-NonCommercial 4.0 License (<https://creativecommons.org/licenses/by-nc/4.0/>) which permits non-commercial use, reproduction and distribution of the work without further permission provided the original work is attributed as specified on the SAGE and Open Access pages (<https://us.sagepub.com/en-us/nam/open-access-at-sage>).

implicated in the development of CMD in diabetes,^{6–8} and we have demonstrated that attenuated endothelium-dependent relaxation and capillary rarefaction in the heart are responsible for the progression of coronary microvascular dysfunction in type 1 diabetic (T1D) mice^{9–12} and type 2 diabetic (T2D) mice.^{13–16} However, the molecular mechanisms by which diabetes leads to CMD through endothelial dysfunction are largely unknown. Consequentially, there are currently no standardized treatment strategies for CMD with or without diabetes, and patients with CMD are commonly treated with cardiovascular medications used for obstructive CAD.¹⁷ Therefore, further understanding of mechanistic details underlying the progression of CMD in diabetes will allow us to develop novel and proper therapeutic approaches for diabetic patients with CMD.

Protein modification with *O*-linked β -N-acetylglucosamine (*O*-GlcNAc) is a post-translational modification at serine and threonine residues in proteins.¹⁸ Two regulatory enzymes are involved in this modification: *O*-GlcNAc transferase (OGT) and *O*-GlcNAcase (OGA), which catalyze the addition and removal of *O*-GlcNAc from proteins, respectively.¹⁸ It has been known that increased protein *O*-GlcNAcylation is implicated in the development of various diabetic vascular complications.¹⁹ Hyperglycemia induces *O*-GlcNAcylation of endothelial nitric oxide synthase (eNOS) at Ser¹¹⁷⁷, leading to a decrease in nitric oxide (NO) production.²⁰ Rats fed with a high-sugar diet exhibit increased *O*-GlcNAcylation of eNOS in the perivascular adipose tissue (PVAT) that causes PVAT dysfunction.²¹ Zhang et al.²² showed that hyperglycemia increases the expression of intracellular adhesion molecule 1 in retinal endothelial cells (ECs) through *O*-GlcNAcylation of Sp1 (specificity protein 1), resulting in retinal damage seen in diabetic retinopathy. It has also been shown that the upregulation of angiopoietin 2 (Ang-2) upon Nucleoside diphosphate kinase B depletion in ECs is mediated by *O*-GlcNAcylation of FoxO1, a transcription factor that regulates Ang-2; thus, driving the development of diabetic retinopathy.²³ *O*-GlcNAcylation of Akt at Thr⁴³⁰ and Thr⁴⁷⁹ in aortic smooth muscle cells is significantly increased in T1D mice, which results in increased Runx2 expression by Akt activation and subsequent induction of smooth muscle cell calcification.²⁴ We demonstrated that *O*-GlcNAcylation of connexin 40 reduces intracellular gap junction communication, leading to impairment of endothelium-dependent hyperpolarization-mediated relaxation in coronary arteries of T1D mice.¹¹ Our recent report showed that increased p53 *O*-GlcNAcylation in Tallyho mice (spontaneous T2D mice) is involved in increased endothelial apoptosis and decreased capillary density in the heart.¹⁶ Despite the vast array of protein *O*-GlcNAcylation research, few reports investigate the pathophysiological role

of protein *O*-GlcNAcylation in CECs in diabetes-induced CMD.

Diabetic mouse models are essential for investigating molecular mechanisms of diabetes-related cardiovascular disease. There are several genetically modified or spontaneous T2D mice (e.g., Lept^{db/db}, KK-A^y, Tallyho),²⁵ and their metabolic parameters are well characterized. A disadvantage of those mice is it would take some time to develop gene knock-in or knock-out mice with their background. Therefore, an inducible T2D mouse model would be ideal for the experiments in transgenic mice. Type 2 diabetes can be induced in mice by a high-fat diet (HFD) feeding paired with a single intraperitoneal injection of low-dose streptozotocin (STZ). This mouse model exhibits hyperglycemia, hyperinsulinemia, increased body weight, abnormal glucose tolerance, insulin resistance, and dyslipidemia^{13–15,25–30}; this is a well-established animal model for T2D study, and the metabolic characteristics are very close to those in human type 2 diabetes induced by Western-diet.^{25,31–34} In our lab, feeding mice with HFD alone does not induce stable type 2 diabetes in mice but does lead to obesity and insulin resistance; however, a low-dose STZ injection (75 mg/kg, i.p.) with HFD enables us to generate a reproducible T2D mice.^{13–15,26,29,30}

This study examines whether and how excess protein *O*-GlcNAcylation in cardiac endothelial cells (CECs) regulates coronary microvascular function in inducible T2D mice generated by HFD with low-dose STZ injection. Our data demonstrate that OGA overexpression in T2D mice decreases protein *O*-GlcNAcylation in CECs, which subsequently reduces endothelial apoptosis, increases capillary density in the heart, and restores coronary microvascular function, evidenced by increased CFVR. Improving coronary microvascular function by overexpression of OGA in ECs also ameliorates cardiac contractility in inducible T2D mice. These data suggest that OGA is a potential therapeutic target for CMD in diabetic patients.

Materials and methods

Chemical agents

Chemicals and antibodies were obtained from the following companies: anti-*O*-GlcNAc antibody (RL2) from Abcam (Cambridge, MA, USA); anti-Actin from Cell Signaling (Danvers, MA, USA); anti-CD31 from BD Biosciences (San Jose, CA, USA); medium 199, streptomycin/penicillin, trypsin/EDTA, endothelial cell growth supplement, fetal bovine serum, sheep anti-rat IgG Dynabeads®, Matrigel, DiI-acLDL, and Hoechst 33342 from Thermo Fisher Scientific (Waltham, MA, USA); collagenase II and dispase II from Worthington Biochemical Corp. (Lakewood, NJ, USA); STZ from Enzo Life Sciences, Inc. (Farmingdale, NY, USA); and

O-(2-acetamido-2-deoxy-D-glucopyranosylidene) amino N-phenylcarbamate from Toronto Research Chemicals (North York, ON, Canada). Any other chemicals were purchased from Sigma-Aldrich Inc. (St. Louis, MO, USA).

Animals

The Institutional Animal Care and Use Committee (IACUC) at both the University of California, San Diego (UCSD, protocol number S18185) and the University of Arizona (UA, protocol number 14-520) approved experimental protocols used in this study. All laboratory personnel who performed animal experiments received the required training. This study was organized to comply with the US government regulations involving laboratory animal use. The University has been certified by PHS with Animal Welfare Assurance numbers A3033-01 (UCSD) and A3248-01 (UA). The total mouse number used in this experiment is 111 mice.

The mouse strain that overexpresses OGA in ECs was generated in our laboratory previously.¹¹ Briefly, mice carrying the Tie2 promoter with reverse tetracycline-controlled transactivator gene (the Jackson Laboratory, strain #005493, C57BL/6 background) were crossed with the mouse with a tetracycline response element followed by OGA gene (background: C57BL/6). The primer sequence information for genotyping is listed in [Supplemental Table 1](#). Male double-transgenic mice were randomly separated into three groups: control, diabetic, and OGA-overexpressed diabetic mice. T2D was induced in double transgenic mice at 6 weeks of age by STZ injection (75 mg/kg, dissolved in citrate buffer, i.p.) and fed a HFD (60% kcal) after injection.^{13,14} At 16 weeks of age, OGA overexpression was achieved by doxycycline (DOX) administration in drinking water (0.2 mg/mL) for 6 weeks. Mice were used for experiments at 22 weeks old. An oral glucose tolerance test (OGTT) was performed, as described previously, in order to determine T2D phenotype.¹⁶ Heart dissection was performed under anesthesia with a mixture of ketamine (100 mg/kg, i.p.) and xylazine (5 mg/kg, i.p.). All efforts were made to minimize suffering from pain.

Isolation of mouse CECs

Isolation of mouse CECs was performed using previously described method.^{9–16,35} Briefly, heart tissues were minced and incubated with M199 containing 1 mg/mL collagenase II and 0.6 U/ml dispase II for 1 h at 37°C with occasional agitation. Single suspended cells were then incubated with CD31-precoated Dynabeads for 1 h at 4°C. A purity test was conducted by assessing Dil-acLDL uptake, a marker for living ECs, and staining with endothelial surface marker, *Bandeiraea Simplicifolia* Lectin- FITC (BS-I). The population of cells was also co-stained with Hoechst 33342 (a

nuclear staining marker) to count the total cell number. Efficient isolation yields approximately 10⁴ cells from one heart with over 80% purity.

Western blot analysis

Western Blot was conducted using SDS-PAGE and an electrophoretic transfer to nitrocellulose membranes. The following primary antibodies were used: RL2 (an anti-*O*-GlcNAc antibody, 1:5000, Abcam, #AB2739) and anti-actin (a loading control, 1:5000, Cell Signaling, #4968). RL2 binds to *O*-GlcNAc and is used to detect protein *O*-GlcNAcylation. The levels of protein *O*-GlcNAc modification are presented with the sum of intensity from the entire signal and bands, which give strong signals to confirm the trend of change.

Coronary flow velocity reserve measurement

Coronary microvascular function was determined by assessment of coronary flow velocity reserve (CFVR).^{14,16} Coronary blood flow velocity (CFV) was measured by echocardiography using a Vevo2100 system (FUJIFILM Visual Sonics, Inc., Toronto, Canada). Mice were anesthetized with isoflurane (1%), and the resting level of CFV was obtained. CFVR was defined as the ratio of the maximal hyperemic CFV (induced by 2.5% isoflurane) divided by the resting CFV (1% isoflurane).

Analysis of capillary density and EC apoptosis in the left ventricle

We evaluated capillary density and EC apoptosis in the left ventricle (LV) as previously described.^{10–12,14–16} Briefly, heart tissue sections (6 µm in thickness) were co-stained with BS-Lectin-FITC (an EC marker) and TUNEL-TRITC (an apoptotic marker). The images were captured with a Nikon Eclipse Ti-E microscope (Nikon Corp. Tokyo, Japan) with a ×20 objective lens. Cells stained with both BS-Lectin-FITC and TUNEL-TRITC were determined as apoptotic endothelial cells.

Hemodynamic studies

Mice were anesthetized with isoflurane on the heating pad. A pressure-volume loop catheter (PVR-1030, Millar Instruments, Houston, TX, USA) was inserted into the right carotid artery and progressed further into the LV.¹⁶ Hemodynamic parameters were measured using an MPVS Ultra system (Millar Instruments). These parameters were then recorded by Lab Chart Pro 8 (AD Instruments Inc., Colorado Springs, CO, USA).

High glucose treatment and OGA gene transduction in human CECs

High glucose (HG) treatment was achieved in human CECs (Lonza Group AG, Basel, Switzerland) by adding 20 mmol/L glucose to the EC media, creating a final glucose concentration of 25 mmol/L. Mannitol (an osmotic control) was added at the same concentration, creating a final glucose concentration of 5 mmol/L (normal glucose [NG]). Human CECs were incubated in HG- or NG-containing media for 4 days. OGA adenovirus (OGA-Adv) was transduced in CECs in order to overexpress OGA gene. Control or OGA-Adv was added at 100 pfu/cell. Gene transduction was achieved 1 day before initiating HG treatment.

Ex vivo angiogenesis assay in human CECs

We coated a 4-well chamber with Matrigel and plated CECs at 4×10^4 cells per well. After 24 h of incubation, four microscopic fields were randomly selected and photographed with a 4x objective lens using an EVOS FL Auto Cell Imaging System (Thermo Fisher Scientific Inc.). Total tube length, junction number, and node number were analyzed using NIH ImageJ 1.5k software.¹⁴

Ex vivo apoptosis detection assay in human CECs

Human CECs were plated in a 24-well chamber with a glass bottom at 2×10^4 cells per well. After gene transduction and NG- or HG-treatment, cells were stained with annexin V/ANXA5-FITC apoptosis detection reagent (Abcam) and Hoechst 33342. Randomly selected five microscopic fields/well were imaged with a $\times 20$ objective lens using EVOS FL Auto Cell Imaging System. The ratio of annexin V positive cell number to total cell number was used to display the effect of OGA on endothelial apoptosis.

Real-time PCR

We used real-time PCR to measure mRNA levels of different genes in mouse CECs. A miRNeasy Mini Kit (QIAGEN, Chatsworth, CA, USA) was used to isolate mRNA. A custom qPCR array plate (384-well plate) was made by QIAGEN Inc. to determine expression levels of 92 genes in four groups at once (SABIO Number CAPA38128-6:CLAM25240). We selected the genes that play crucial roles in endothelial function, such as a) endothelial angiogenesis, b) endothelium-dependent relaxation and contraction, c) Ca^{2+} homeostasis, and d) mitochondria-mediated apoptosis (See [Supplemental Table 2](#) for the gene list). qPCR was conducted using the CFX384 Touch Real-Time PCR Detection System (Bio-Rad Laboratories, Hercules, CA, USA). GAPDH was used as an internal control. The transcript levels of the gene

of interest were quantified according to the cycle threshold (ΔCt) method. Ct values >35 were not included in the analysis and were considered negative.

Data and statistical analysis

Data analysis was conducted in a blinded manner whenever possible. All experimental plans included proper controls matched to the experimental groups. The figure legend describes mouse numbers and independent experiment numbers (n). Statistical analysis was performed using GraphPad Prism 9.1 (La Jolla, CA, USA). Data in the figures of the results section are represented as mean \pm SEM. One-way ANOVA (except [Figure 1\(d\)](#)) was used to compare multiple groups with Bonferroni *post hoc* analysis. Differences were considered to be statistically significant when $p < 0.05$. In [Figure 1\(d\)](#), we used two-way ANOVA with Bonferroni *post hoc* analysis. The qPCR data in [Figure 6](#) were subjected to Grubbs' test to mathematically remove the outliers caused by technical errors. To analyze the data within narrow distributions, we used 0.1 to obtain Grubbs' critical value (1.83 for $n = 7$ [Cont, T2D] and 1.73 for $n = 6$ [T2D + DOX]). After eliminating the outliers, the data were analyzed using one-way ANOVA with Bonferroni *post hoc* analysis.

Results

OGA overexpression decreased protein O-GlcNAcylation modification in CECs of diabetic mice without changing glucose tolerance, body weight, and plasma cholesterol levels

[Figure 1\(a\)](#) demonstrates the sequence of T2D induction and DOX administration in mice. OGA is the enzyme that removes O-GlcNAc from the proteins.¹⁸ First, we examined whether DOX-induced OGA overexpression altered protein O-GlcNAcylation levels in diabetic mice. Mouse CECs were isolated from three groups, and the level of protein O-GlcNAc modification was detected by RL2 antibody. Protein O-GlcNAcylation was increased in diabetic mice, and OGA overexpression significantly decreased the levels of O-GlcNAc protein modification in CECs of T2D mice ([Figure 1\(b\) and \(c\)](#)). T2D mice exhibited abnormal glucose tolerance ([Figure 1\(d\) and \(e\)](#)) and significant increases in body weight ([Figure 1\(f\)](#)) and total cholesterol ([Figure 1\(g\)](#)) compared to the control mice. OGA overexpression by DOX administration did not affect glucose tolerance, body weight, and cholesterol level when compared to T2D mice ([Figure 1\(d\)–\(g\)](#)). These data suggest that OGA overexpression successfully reduced protein O-GlcNAcylation in ECs of T2D mice without altering glucose hemodynamics in the body.

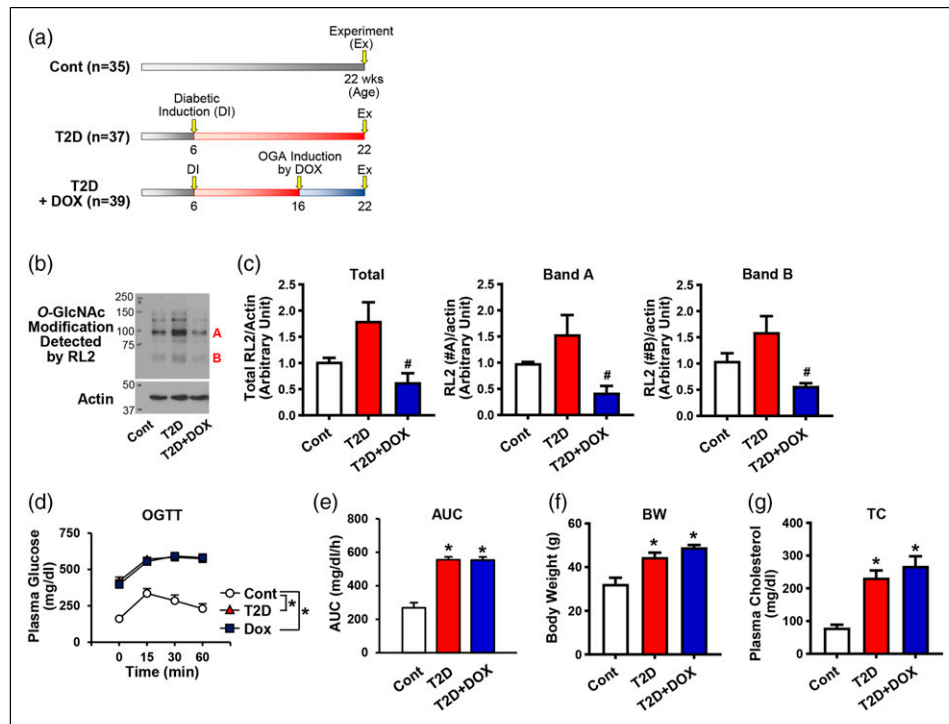


Figure 1. Phenotypic characteristics of control, T2D, and OGA-overexpressed T2D mice. (a): Timeline of diabetic induction and OGA gene overexpression. (b): Representative Western Blot image of O-GlcNAc protein modification detected by RL2 and actin levels in mouse cardiac endothelial cells (CECs) from control, T2D, and T2D + DOX mice. (c): Summarized data of protein O-GlcNAcylation. Left: Total RL2 protein levels. $N_{\text{mice}} = 4$ in each group. Middle: RL2 protein levels at the band A. $N_{\text{mice}} = 4$ in each group. Right: RL2 protein levels at the band B. $N_{\text{mice}} = 4$ in each group. RL2 signals were normalized by actin signal. (d): Oral glucose tolerance test (OGTT). Control, Cont, $n_{\text{mice}} = 8$; T2D, $n_{\text{mice}} = 10$; T2D with OGA induction (T2D + DOX), $n_{\text{mice}} = 10$. Two-way ANOVA was conducted to assess the statistical significance between the three groups. (e): Area under the curve (AUC) of OGTT. Cont, $n_{\text{mice}} = 8$; T2D, $n_{\text{mice}} = 10$; T2D + DOX, $n_{\text{mice}} = 10$. (f): Body weight (BW). Cont, $n_{\text{mice}} = 8$; T2D, $n_{\text{mice}} = 10$; T2D + DOX, $n_{\text{mice}} = 10$. (g): Total cholesterol (TC). $N_{\text{mice}} = 4$ per group. Data are shown as mean \pm SEM. * $p < 0.05$ vs. Cont. # $p < 0.05$ vs. T2D. One-way ANOVA (in c and e–g) was used to determine statistical significance between experimental groups with Bonferroni *post hoc* test.

OGA overexpression restored coronary microvascular function by improving capillary density and decreasing EC apoptosis in the heart of diabetic mice

To examine whether our T2D mice have CMD and if OGA overexpression restores coronary microvascular function, we measured CFVR as a surrogate parameter of coronary microvascular function.^{36,37} Compared to control mice, T2D mice displayed a significant reduction in CFVR (Figure 2(a) and (b)). Supplemental Figure 1 demonstrates that our T2D mice do not show any lipid plaque formation; therefore, the decrease in CFVR is solely due to attenuated coronary microvascular function in T2D mice. Decreased CFVR was significantly increased by OGA overexpression in T2D mice (Figure 2(a) and (b)). There was no difference in the baseline of CFV among the three groups (Cont, 552.8 ± 54.3 ; T2D, 737.8 ± 72.5 ; T2D + DOX, 523.1 ± 74.0). The change in capillary density in the LV influences CFVR,^{38,39} therefore, we assessed and compared capillary density in

control, diabetic and diabetic mice treated with DOX. T2D mice exhibit lower capillary density than control mice, while OGA overexpression significantly increased capillary density in T2D mice (Figure 2(c) and (d)). Capillary density is regulated by endothelial apoptosis, endothelial migration and proliferation, and incorporation of circulating endothelial progenitor cells into the sites where ECs are damaged. Figure 2(e) and (f) demonstrate that the number of apoptotic ECs was significantly increased in T2D mice compared to control mice, whereas OGA overexpression in T2D mice showed a decrease in endothelial apoptosis.

Restoration of coronary microvascular function improved cardiac contractility in T2D mice

It has been reported that sustained reduction of coronary flow leads to attenuated cardiac contractility.^{40,41} Therefore, we assessed cardiac function by inserting the catheter in the LV. T2D mice exhibited significant impairment of

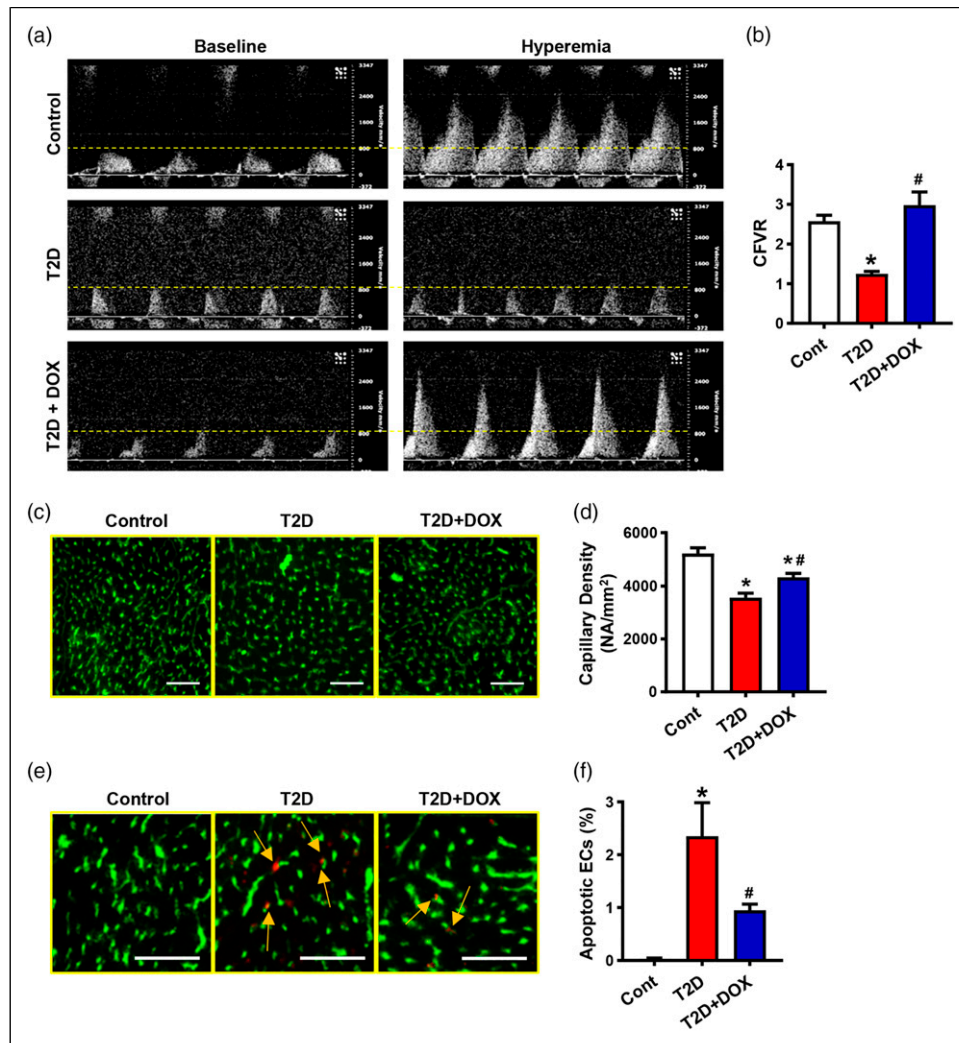


Figure 2. Effect of OGA overexpression on coronary flow velocity reserve, capillary density, and endothelial apoptosis in T2D mice. (a): Representative image of coronary flow. **Left:** coronary flow at the baseline (1% isoflurane). **Right:** coronary flow at hyperemia (2.5% isoflurane). The height shows the velocity of the flow (yellow line). (b): Summarized data of coronary flow velocity reserve (CFVR). Cont, $n_{\text{mice}} = 7$; T2D, $n_{\text{mice}} = 7$; T2D + DOX, $n_{\text{mice}} = 8$. (c): Representative photomicrographs displaying capillary density of the LV. Endothelial cells (ECs) were stained with BS-lectin-FITC. Bar = 50 μm . (d): Summarized data of capillary density. Cont, $n_{\text{mice}} = 4$; T2D, $n_{\text{mice}} = 4$; T2D + DOX, $n_{\text{mice}} = 5$. (e): Representative photomicrograph of apoptotic ECs. ECs were stained with lectin-FITC (green) and TUNEL-TRITC (red). Orange arrows point to co-stained cells that exhibit EC apoptosis. Bar = 50 μm . (f): Summarized data of apoptotic ECs (the number of apoptotic ECs divided by the total number of EC). Cont, $n_{\text{mice}} = 4$; T2D, $n_{\text{mice}} = 4$; T2D + DOX, $n_{\text{mice}} = 5$. Data are shown as mean \pm SEM. * $p < 0.05$ vs. Cont. # $p < 0.05$ vs. T2D. One-way ANOVA was used to determine statistical significance between experimental groups with Bonferroni *post hoc* test.

cardiac output (CO), left ventricular systolic pressure (LVSP), dp/dt max, dp/dt min, and ejection fraction (EF) without affecting mean arterial pressure and heart rate (Figure 3). Strikingly, OGA overexpression significantly improved cardiac contractility in T2D mice. The results in Figure 2 and 3 indicate that OGA overexpression restores coronary microvascular function by increasing capillary density and CFVR, which subsequently augments cardiac contractility in diabetic mice.

OGA overexpression increased capillary network formation in human CECs treated with high glucose

An ex vivo capillary network formation was conducted in order to investigate how OGA overexpression influences endothelial angiogenic capacity under high glucose conditions. The microphotographs and summarized data showed attenuated capillary network formation in HG-treated human CECs, and OGA overexpression in HG-

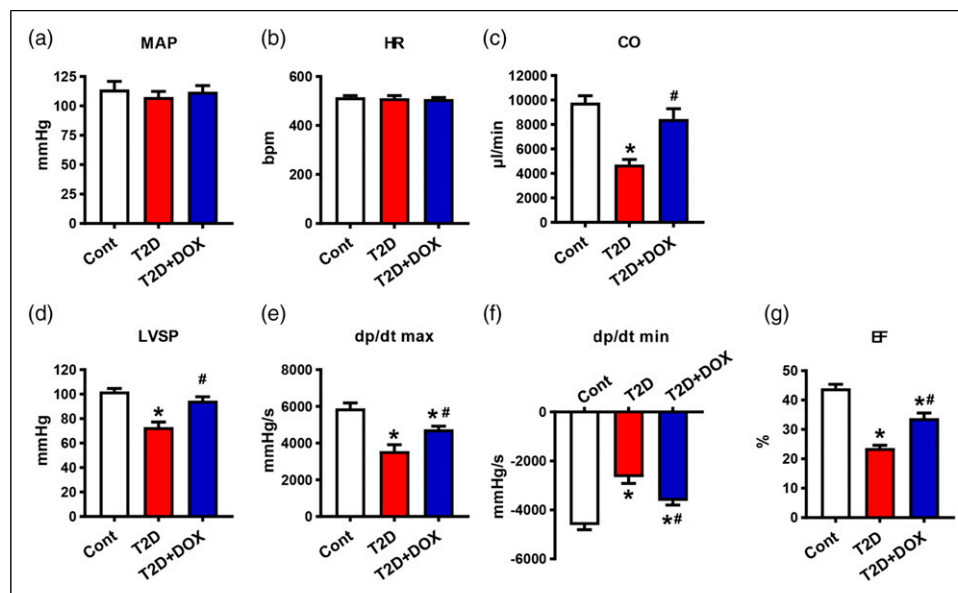


Figure 3. Cardiac hemodynamic features of control mice, T2D mice, and OGA overexpressing T2D mice. (a): Mean arterial pressure (MAP). (b): Heart rate (HR). (c): Cardiac output (CO). (d): Left ventricular systolic pressure (LVSP). (e): dp/dt max. (f): dp/dt min, (g): Ejection fraction (EF). Cont, $n_{mice} = 5$; T2D, $n_{mice} = 5$; T2D + DOX, $n_{mice} = 6$. Data are shown as mean \pm SEM. * $p < 0.05$ vs. Cont. # $p < 0.05$ vs. T2D. One-way ANOVA was used to determine statistical significance between experimental groups with Bonferroni *post hoc* test.

treated CECs partially, but significantly, restored capillary network formation (Figure 4). OGA overexpression in NG-treated CECs did not influence capillary network formation (Supplemental Figure 2). HG-treated CECs displayed a drastic increase in endothelial apoptosis compared to normal glucose conditions. In contrast, OGA overexpression showed a trend of decrease in apoptotic ECs without significant difference (Figure 5). These data suggest that high-glucose treatment reduces capillary network formation through excess protein *O*-GlcNAcylation.

OGA overexpression altered mRNA levels of *Sp1* and *MAPK1* in mouse CECs of T2D mice

Other investigators and we demonstrated that OGA overexpression increases target proteins' activities by removing *O*-GlcNAc residues.^{11,16,42} However, there are few reports examining the effect of OGA overexpression on mRNA expression levels. We here measured and compared the mRNA levels of 92 genes in mouse CECs isolated from control mice, T2D mice, and T2D mice treated with DOX using a qPCR. Of 92 genes, seven displayed significant differences in mRNA levels among three groups: *Dnm1l*, *Flt4*, *Kcnn3*, *Mapk1*, *Pecam1*, *Sp1*, and *Vcam1*. Within seven genes, two genes, *Mapk1* and *Sp1*, showed increased mRNA expression in mouse CECs of OGA-overexpressed T2D mice compared to CECs from T2D mice. These data suggest that *Sp1* and *Mapk1* might be involved in

O-GlcNAcylation-dependent regulation of coronary microvascular function.

Discussion

There has been much discussion of the urgent need to develop specific treatments for CMD patients due to the increasing prevalence of CMD. Importantly, T2D diabetic patients are more prone to CMDs,⁴³⁻⁴⁵ and cardiac mortality is higher in diabetic patients with CMD than control subjects with CMD.¹ Therefore, we investigate the molecular mechanisms of CMD in diabetes. In this study, we used an inducible T2D mouse model, generated by the single administration of a low dose of STZ paired with HFD. Many investigators, including us, have reported this mouse model having hyperglycemia, abnormal glucose tolerance, increased body weight, and dyslipidemia (Figure 1).^{13-15,25-34} Coronary flow reserve (CFR) is a clinically accepted assessment for coronary microvascular function in patients without detectable stenosis in the coronary vasculature. In this study, we used CFVR, instead of CFR, because of the difficulty in determining the precise diameter of the coronary artery, which is required for the calculation of coronary flow. It has been reported that CFVR correlates well with CFR and is a useful surrogate assessment for coronary microvascular function.^{36,37} Inducible T2D mice in C57 background strain hardly develop lipid plaque formation at the age that we used

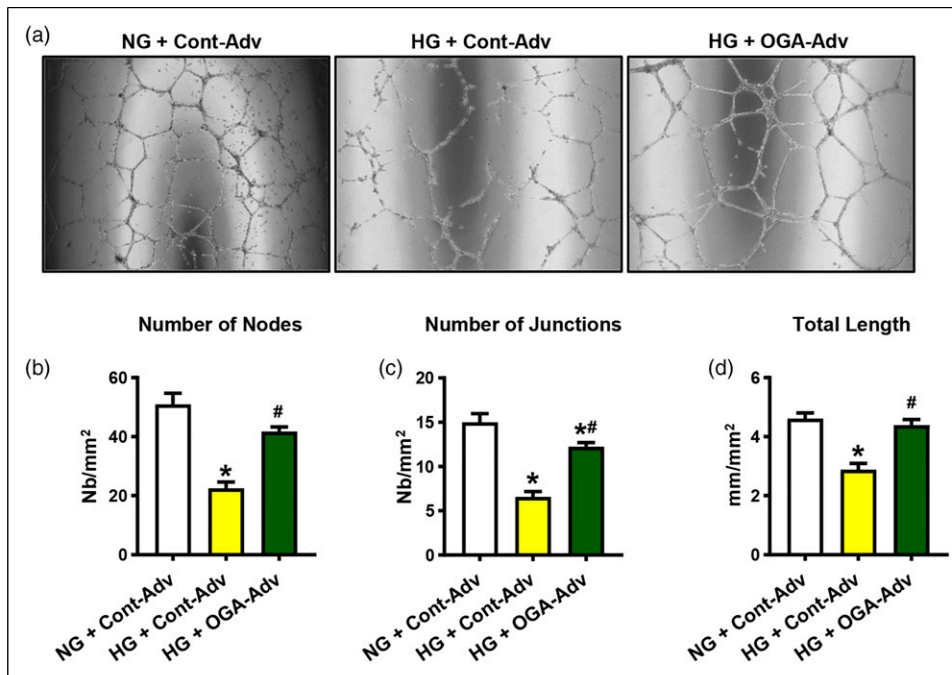


Figure 4. Effects of OGA overexpression on capillary network formation in high-glucose treated human CECs. (a): Representative microphotograph of capillary network formation in human CECs. (b–d): Summarized data of capillary network formation. (b): Number of nodes. (c): Number of junctions. (d): Total length. Human CECs were treated with normal glucose (NG) or high glucose (HG) for 96 h with or without OGA overexpression by OGA-Adv (100 pfu/cell). $N_{\text{experiment}} = 6$ per group. Data are shown as mean \pm SEM. * $p < 0.05$ vs. NG + Cont-Adv. # $p < 0.05$ vs. HG + Cont-Adv. One-way ANOVA was used to determine statistical significance between experimental groups with Bonferroni *post hoc* test.

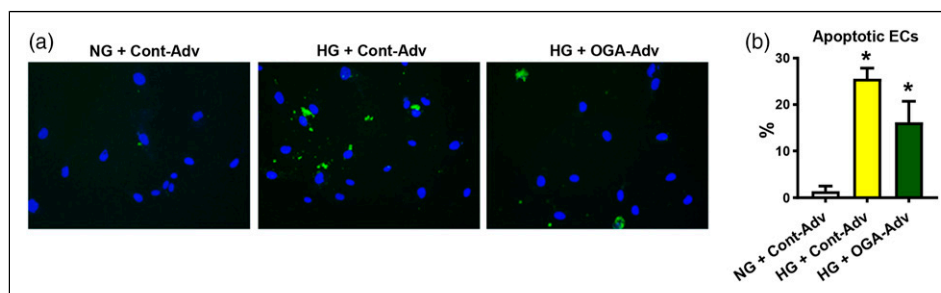


Figure 5. Effect of OGA overexpression on endothelial apoptosis in HG-treated human CECs. (a): Representative microphotograph of apoptosis in human CECs. (b): Summarized data of apoptosis in CECs in NG or HG treatment with or without OGA overexpression. $N_{\text{experiment}} = 5$ for each group. Cell apoptosis was determined by Annexin-V. Data are shown as mean \pm SEM. * $p < 0.05$ vs. NG + Cont-Adv. # $p < 0.05$ vs. HG + Cont-Adv. One-way ANOVA was used to determine statistical significance between experimental groups with Bonferroni *post hoc* test.

(Supplemental Figure 1); therefore, the reduction of CFVR seen in T2D mice is primarily caused by attenuated coronary microvascular function (Figure 2(b)). Endothelial dysfunction is implicated in coronary microvascular dysfunction in CMD.^{38,39,46–49} Reduced endothelium-derived relaxing factors, attenuated endothelium-derived hyperpolarization, and/or increased endothelium-derived contracting factors lead to narrowing the diameter of coronary arteries and arterioles that subsequently reduces coronary

flow in microvascular circulation.⁴⁶ In addition, enhanced coronary endothelial apoptosis and decreased regeneration of new capillaries result in capillary rarefaction in the heart and reduced blood flow in the coronary microcirculation.^{38,39} Other investigators and we reported that capillary density is decreased in the heart of patients and mice suffering from diabetes,^{10,14,16,50–53} and protein *O*-GlcNAcylation in CECs is increased in inducible T1D and spontaneous T2D diabetic mice.^{11,16} Therefore, in this study, we aim to

examine the link between *O*-GlcNAcylation and coronary microvascular dysfunction in inducible T2D mice, which has never been investigated.

In order to examine the role of *O*-GlcNAcylation on diabetic endothelial function, we induced T2D in an endothelium-specific tet-inducible OGA overexpressing mouse model. Excess protein *O*-GlcNAcylation causes maladaptive effects on endothelial migration, proliferation, and survival mice.^{11,16,54} However, it has to be noted that protein *O*-GlcNAcylation is pivotal in physiological function in various cell types.^{55–58} Therefore, it is critical not to “remove” protein *O*-GlcNAcylation, but to reduce *O*-GlcNAcylation levels toward the control range (Figure 1(g)). Tissue-specific OGA overexpression can minimize unwelcome effects on other cell types, and the tet-inducible model allows us to avoid the impact of OGA overexpression during embryonic development. Therefore, our endothelial-specific tet-inducible OGA overexpression mice are well suited to this study. OGA overexpression did not alter fasting glucose level, glucose tolerance, body weight, or dyslipidemia in our inducible T2D mice (Figure 1(d)–(g)), indicating that overexpression of OGA does not alter phenotypic characters of T2D. This also evidences that OGA is restrictedly increased in ECs but not in other cell types. It has been reported that reduction of protein *O*-GlcNAcylation in skeletal muscles^{59,60} in HFD-fed mice improves glucose tolerance, and OGA deletion in β -cells⁶¹ or oocytes⁶² leads to impaired glucose tolerance.

OGA-overexpression in T2D mice restored CFVR to control levels, accompanied by increased capillary density and decreased apoptotic ECs in the LV (Figure 2). These data suggest excess *O*-GlcNAcylation increases apoptotic ECs, followed by decreased capillary density and reduced CFVR. The results align with our previous publications that examined the role of *O*-GlcNAcylation in maintaining capillary density.^{11,16} EC-specific OGA overexpression increased capillary density in the LV of inducible T1D mice generated by an intravenous injection of high-dose STZ (133 mg/kg).¹¹ Overexpression of OGA in Tallyho mice (spontaneous T2D mice) showed restorative effects on CFVR and capillary density.¹⁶ We here confirm that the beneficial effects of OGA overexpression or reduction of protein *O*-GlcNAcylation on cardiac endothelial function are universal phenomena across different types of diabetes.

Coronary microvascular dysfunction not only increases cardiac mortality but also leads to heart failure with preserved EF.^{63,64} However, it has been reported that prolonged reduction of coronary flow results in reduced cardiac contractility.^{40,41} In our diabetic mice, cardiac contractility was significantly attenuated (Figure 3), which might be led by both hyperglycemia-induced cardiac myocyte dysfunction and sustained blood flow reduction because of attenuated coronary microvascular function by hyperglycemia. OGA overexpression in ECs significantly

increased cardiac contractility in T2D mice due partly to increased capillary density, followed by enhanced oxygen delivery to cardiac myocytes. It has to be noted that dp/dt max, dp/dt min, and EF were augmented but not fully recovered toward the control range. Hu et al.⁶⁵ showed that overexpression of OGA in cardiac myocytes significantly augmented cardiac contractility in inducible T1D mice. These data suggest that improving coronary microvascular function has a beneficial effect on restoring cardiac function in diabetes; however, full recovery of cardiac contractility requires further improvement in cardiac myocytes of diabetic mice.

Capillary density is modified by endothelial function; increased endothelial apoptosis reduces capillary density in the heart. If resident ECs can actively migrate and proliferate and/or endothelial progenitor cells can sufficiently adhere and home to damaged vascular walls, capillary density might not be dramatically reduced even though endothelial apoptosis is enhanced. Our diabetic mice exhibit hyperglycemia and dyslipidemia. To investigate whether hyperglycemia alters capillary density through excess protein *O*-GlcNAcylation, we treated human CECs with HG and examined the effect of OGA on endothelial function ex vivo. We found that capillary network formation was significantly attenuated by HG treatment, and OGA overexpression in HG-treated ECs exhibited significant restoration of capillary network formation toward levels similar to NG-treated ECs (Figure 4). Interestingly, overexpression of OGA in NG-treated ECs did not alter capillary network formation (Supplemental Figure 2), suggesting that an increase in OGA expression above physiological does not lead to pathophysiological angiogenesis, like cancer cells. Matrigel-based capillary network formation assay (also known as tube formation assay and/or angiogenesis assay) is a useful tool to evaluate endothelial angiogenic capability.^{66,67} Attenuated angiogenesis is a hallmark of diabetic angiopathy, and it has been reported that HG treatment decreases capillary network formation in most ECs isolated from different vessels, including coronary ECs,^{10,68} but increases in retinal ECs.^{69,70} Other investigators and we reported that decreased angiogenic capacity by HG treatment or hyperglycemia might be caused by increased *O*-GlcNAcylation of Akt,⁵⁴ GFAT1,⁷¹ Cx40,¹¹ and p53.¹⁶ Akt, GFAT1, and Cx40 are involved in endothelial migration, while p53 can modify angiogenic capacity through the activation of cell apoptosis.

Figure 5 shows that HG treatment in human CECs significantly increased endothelial apoptosis, which is in line with other reports.^{16,72,73} OGA-Adv transduction in HG-treated CECs showed a trend of decrease in apoptotic ECs; however, there was no significant difference in apoptotic endothelial population between control-Adv-transduced ECs and OGA-Adv-transduced ECs under

high glucose conditions (Figure 5). Chronic OGA overexpression in T2D mice significantly decreased endothelial apoptosis (Figure 2(e)), but OGA overexpression did not affect endothelial apoptosis in HG-treated CECs in ex vivo, which would be partially due to the shorter duration of OGA overexpression (5 days) than in vivo experiment (6 weeks).

To identify key genes that may contribute to the restorative effects seen by OGA-overexpression in T2D mice, we used a custom PCR array to determine altered gene expression levels in mouse CECs isolated from control, T2D, and EC-specific OGA-overexpressing T2D mice. Among 92 genes, only seven genes had a significant difference with ANOVA, and two genes, *Sp1* and *Mapk1*, showed to be upregulated by OGA-overexpression. *Sp1* is a transcription factor that regulates expression levels of many genes, including angiogenesis-related genes (e.g., *Akt*, *Fgf*, *Pdgf*, *Vegfb*) and transcription factors (e.g., *p53*, *Sp1*, *Runx*), and its activity is heavily regulated by post-translational modification.⁷⁴ Hyperglycemia and/or high glucose treatment decrease *Sp1* expression levels in coronary ECs¹⁰ but increase in retinal ECs,⁷⁵ implying that the change in *Sp1* levels might participate in diabetes-mediated vascular complications. *Sp1* leads to angiogenesis,⁷⁶ therefore, overexpression of *Sp1* by OGA seen in

Figure 6 might be involved in increased capillary density in OGA overexpressing T2D mice (Figure 2(c)) and enhanced capillary network formation in HG-treated CECs (Figure 4). However, it is also noted that excess *Sp1* expression is the cause of tumor angiogenesis⁷⁴ and diabetic retinopathy.⁷⁵ Targeting *Sp1* as a treatment for capillary rarefaction in diabetes is thus questionable. MAPK1 is an enzyme involved in various signaling pathways such as migration, proliferation, and cell cycle.⁷⁷ Although MAPK1 plays a critical role in the physiological function of ECs, overactivation of MAPK1 has been observed in diabetes, resulting in a pathophysiological response of MAPK1 in ECs.⁷⁸⁻⁸⁰ Therefore, it requires further experiments to identify the role of MAPK1 upregulation seen in OGA-overexpressing diabetic mice in coronary endothelial dysfunction.

Protein *O*-GlcNAcylation is regulated by not only OGA but also OGT; therefore, some might wonder whether OGT could be used to modify protein *O*-GlcNAcylation and following events caused by excess *O*-GlcNAcylation in diabetes. Importantly, OGT not only regulates protein *O*-GlcNAcylation but also activates other proteins and expression levels involved in tumor progression. OGT levels are increased in various cancer cells, increasing their migration and proliferation via changing angiogenic peptide

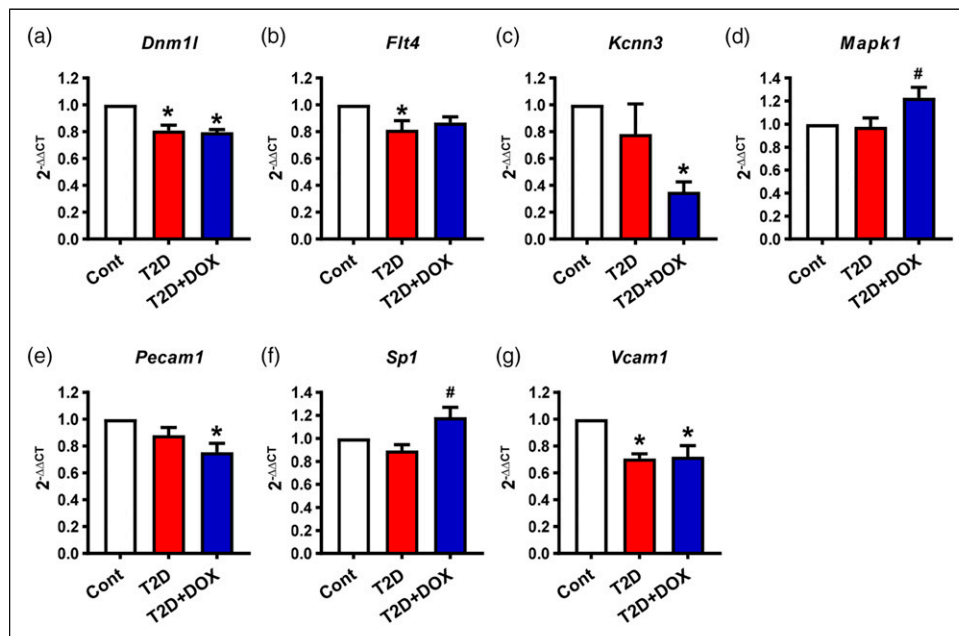


Figure 6. Genes that demonstrate altered mRNA levels in CECs from control, T2D, and OGA overexpressing T2D mice. Gene expression level was determined by a custom PCR Array in 92 genes. (a): *Dnm1l*. Cont, $n_{\text{mice}} = 6$; T2D, $n_{\text{mice}} = 5$; T2D + DOX, $n_{\text{mice}} = 4$. (b): *Flt4*. Cont, $n_{\text{mice}} = 7$; T2D, $n_{\text{mice}} = 6$; T2D + DOX, $n_{\text{mice}} = 5$. (c): *Kcnn3*. Cont, $n_{\text{mice}} = 7$; T2D, $n_{\text{mice}} = 6$; T2D + DOX, $n_{\text{mice}} = 5$. (d): *Mapk1*. Cont, $n_{\text{mice}} = 7$; T2D, $n_{\text{mice}} = 6$; T2D + DOX, $n_{\text{mice}} = 6$. (e): *Pecam1*. Cont, $n_{\text{mice}} = 7$; T2D, $n_{\text{mice}} = 7$; T2D + DOX, $n_{\text{mice}} = 5$. (f): *Sp1*. Cont, $n_{\text{mice}} = 7$; T2D, $n_{\text{mice}} = 6$; T2D + DOX, $n_{\text{mice}} = 6$. (g): *Vcam1*. Cont, $n_{\text{mice}} = 7$; T2D, $n_{\text{mice}} = 5$; T2D + DOX, $n_{\text{mice}} = 5$. Data are shown as mean \pm SEM. * $p < 0.05$ vs. Cont. # $p < 0.05$ vs. T2D. Grubbs' test was carried out to eliminate the outliers first. One-way ANOVA was used to determine statistical significance between experimental groups with Bonferroni *post hoc* test.

concentration.⁸¹ Therefore, we need to be cautious in changing OGT levels in the cells. We have shown that OGT level is not altered in CECs in diabetes;¹¹ consequently, it might not be preferable to regulate OGT levels in CMD in diabetes.

In summary, we identified that overexpression of endothelial OGA exhibits a beneficial effect on coronary endothelial function in inducible T2D diabetic mice by augmenting endothelial angiogenesis and increasing capillary density in the heart, resulting in restoration of CFVR. The improvement of coronary microvascular function also increases cardiac contractility in inducible T2D mice. Therefore, OGA is a promising therapeutic target for CMD in diabetes.

Author contributions

J.C., R.S., and A.T. conducted the experiments, analyzed the data, and drafted and reviewed the manuscript. H.C., J.Y., and W.D. supervised experiments and contributed to the manuscript review. A.M. conceived the project, designed the experiments, analyzed the data, and reviewed and edited the manuscript.

Declaration of conflicting interests

The author(s) declared no potential conflicts of interest with respect to the research, authorship, and/or publication of this article.

Funding

This work was supported by grants from the National Heart, Lung, and Blood Institute of the National Institutes of Health (HL142214, HL146764, and HL154754) and the Department of Defense (W81XWH2110472).

ORCID iD

Ayako Makino  <https://orcid.org/0000-0003-1259-8604>

Supplemental Material

Supplemental material for this article is available online.

References

- Murthy VL, Naya M, Foster CR, et al. Association between coronary vascular dysfunction and cardiac mortality in patients with and without diabetes mellitus. *Circulation* 2012; 126: 1858–1868.
- Erdogan D, Yucel H, Uysal BA, et al. Effects of prediabetes and diabetes on left ventricular and coronary microvascular functions. *Metabolism* 2013; 62: 1123–1130.
- Spoladore R, Fiscicaro A, Faccini A, et al. Coronary microvascular dysfunction in primary cardiomyopathies. *Heart* 2014; 100: 806–813.
- Petersen JW and Pepine CJ. Microvascular coronary dysfunction and ischemic heart disease: where are we in 2014? *Trends Cardiovasc Med* 2015; 25: 98–103.
- Bairey Merz CN, Pepine CJ, Walsh MN, et al. Ischemia and no obstructive coronary artery disease (INOCA): developing evidence-based therapies and research agenda for the next decade. *Circulation* 2017; 135: 1075–1092.
- George PB, Tobin KJ, Corpus RA, et al. Treatment of cardiac risk factors in diabetic patients: How well do we follow the guidelines? *Am Heart J* 2001; 142: 857–863.
- Labazi H and Trask AJ. Coronary microvascular disease as an early culprit in the pathophysiology of diabetes and metabolic syndrome. *Pharmacol Res* 2017; 123: 114–121.
- Kibel A, Selthofer-Relatic K, Drenjancevic I, et al. Coronary microvascular dysfunction in diabetes mellitus. *J Int Med Res* 2017; 45: 1901–1929.
- Estrada IA, Donthamsetty R, Debski P, et al. STIM1 restores coronary endothelial function in type 1 diabetic mice. *Circ Res* 2012; 111: 1166–1175.
- Makino A, Platoshyn O, Suarez J, et al. Downregulation of connexin40 is associated with coronary endothelial cell dysfunction in streptozotocin-induced diabetic mice. *Am J Physiol Cell Physiol* 2008; 295: C221–C230.
- Makino A, Dai A, Han Y, et al. O-GlcNAcase overexpression reverses coronary endothelial cell dysfunction in type 1 diabetic mice. *Am J Physiol Cell Physiol* 2015; 309: C593–C599.
- Sasaki K, Donthamsetty R, Heldak M, et al. VDAC: old protein with new roles in diabetes. *Am J Physiol Cell Physiol* 2012; 303: C1055–C1060.
- Cho YE, Basu A, Dai A, et al. Coronary endothelial dysfunction and mitochondrial reactive oxygen species in type 2 diabetic mice. *Am J Physiol Cell Physiol* 2013; 305: C1033–C1040.
- Si R, Cabrera JTO, Tsuji-Hosokawa A, et al. HuR/Cx40 downregulation causes coronary microvascular dysfunction in type 2 diabetes. *JCI Insight* 2021; 6: e147982.
- Pan M, Han Y, Basu A, et al. Overexpression of hexokinase 2 reduces mitochondrial calcium overload in coronary endothelial cells of type 2 diabetic mice. *Am J Physiol Cell Physiol* 2018; 314: C732–C740.
- Si R, Zhang Q, Tsuji-Hosokawa A, et al. Overexpression of p53 due to excess protein O-GlcNAcylation is associated with coronary microvascular disease in type 2 diabetes. *Cardiovasc Res* 2020; 116: 1186–1198.
- Marinescu MA, Loffler AI, Ouellette M, et al. Coronary microvascular dysfunction, microvascular angina, and treatment strategies. *JACC Cardiovasc Imaging* 2015; 8: 210–220.
- King DT, Males A, Davies GJ, et al. Molecular mechanisms regulating O-linked N-acetylglucosamine (O-GlcNAc)-processing enzymes. *Curr Opin Chem Biol* 2019; 53: 131–144.
- Chen Y, Zhao X and Wu H. Metabolic stress and cardiovascular disease in diabetes mellitus: The role of protein O-GlcNAc modification. *Arterioscler Thromb Vasc Biol* 2019; 39: 1911–1924.
- Du XL, Edelstein D, Dimmeler S, et al. Hyperglycemia inhibits endothelial nitric oxide synthase activity by post-translational modification at the Akt site. *J Clin Invest* 2001; 108: 1341–1348.

21. da Costa RM, da Silva JF, Alves JV, et al. Increased O-GlcNAcylation of endothelial nitric oxide synthase compromises the anti-contractile properties of perivascular adipose tissue in metabolic syndrome. *Front Physiol* 2018; 9: 341.
22. Zhang Y, Qu Y, Niu T, et al. O-GlcNAc modification of Sp1 mediates hyperglycaemia-induced ICAM-1 up-regulation in endothelial cells. *Biochem Biophys Res Commun* 2017; 484: 79–84.
23. Shan S, Chatterjee A, Qiu Y, et al. O-GlcNAcylation of FoxO1 mediates nucleoside diphosphate kinase B deficiency induced endothelial damage. *Sci Rep* 2018; 8: 10581.
24. Heath JM, Sun Y, Yuan K, et al. Activation of AKT by O-linked N-acetylglucosamine induces vascular calcification in diabetes mellitus. *Circ Res* 2014; 114: 1094–1102.
25. Fang JY, Lin CH, Huang TH, et al. In vivo rodent models of type 2 diabetes and their usefulness for evaluating flavonoid bioactivity. *Nutrients* 2019; 11: 530.
26. Pan M, Han Y, Si R, et al. Hypoxia-induced pulmonary hypertension in type 2 diabetic mice. *Pulm Circ* 2017; 7: 175–185.
27. Fricovsky ES, Suarez J, Ihm SH, et al. Excess protein O-GlcNAcylation and the progression of diabetic cardiomyopathy. *Am J Physiol Regul Integr Comp Physiol* 2012; 303: R689–R699.
28. Cividini F, Scott BT, Suarez J, et al. Ncor2/PPAR α -dependent upregulation of MCUb in the type 2 diabetic heart impacts cardiac metabolic flexibility and function. *Diabetes* 2021; 70: 665–679.
29. Han Y, Cho YE, Ayon R, et al. SGLT inhibitors attenuate NO-dependent vascular relaxation in the pulmonary artery but not in the coronary artery. *Am J Physiol Lung Cell Mol Physiol* 2015; 309: L1027–L1036.
30. Yin RY, Xue Y, Hu JR, et al. The effects of diet and streptozotocin on metabolism and gut microbiota in a type 2 diabetes mellitus mouse model. *Food and Agricultural Immunology* 2020; 31: 723–739.
31. Luo J, Quan J, Tsai J, et al. Nongenetic mouse models of non-insulin-dependent diabetes mellitus. *Metabolism* 1998; 47: 663–668.
32. Kusakabe T, Tanioka H, Ebihara K, et al. Beneficial effects of leptin on glycaemic and lipid control in a mouse model of type 2 diabetes with increased adiposity induced by streptozotocin and a high-fat diet. *Diabetologia* 2009; 52: 675–683.
33. Islam MS and Loots DT. Experimental rodent models of type 2 diabetes: a review. *Methods Find Exp Clin Pharmacol* 2009; 31: 249–261.
34. Reuter T. Diet-induced models for obesity and type 2 diabetes. *Drug Discovery Today: Disease Models* 2007; 4: 3–8.
35. Luo S, Truong AH and Makino A. Isolation of mouse coronary endothelial cells. *J Vis Exp* 2016; 113: e53985.
36. Gan LM, Wikstrom J and Fritsche-Danielson R. Coronary flow reserve from mouse to man—from mechanistic understanding to future interventions. *J Cardiovasc Transl Res* 2013; 6: 715–728.
37. Wikstrom J, Gronros J and Gan LM. Adenosine induces dilation of epicardial coronary arteries in mice: relationship between coronary flow velocity reserve and coronary flow reserve *in vivo* using transthoracic echocardiography. *Ultrasound Med Biol* 2008; 34: 1053–1062.
38. Tsagalou EP, Anastasiou-Nana M, Agapitos E, et al. Depressed coronary flow reserve is associated with decreased myocardial capillary density in patients with heart failure due to idiopathic dilated cardiomyopathy. *J Am Coll Cardiol* 2008; 52: 1391–1398.
39. Ganz P and Hsue PY. Assessment of structural disease in the coronary microvasculature. *Circulation* 2009; 120: 1555–1557.
40. Selthofer-Relatic K, Mihalj M, Kibel A, et al. Coronary microcirculatory dysfunction in human cardiomyopathies: a pathologic and pathophysiologic review. *Cardiol Rev* 2017; 25: 165–178.
41. Spoladore R, Fisticaro A, Faccini A, et al. Coronary microvascular dysfunction in primary cardiomyopathies. *Heart* 2014; 100: 806–813.
42. Wang Z, Udeshi ND, Slawson C, et al. Extensive crosstalk between O-GlcNAcylation and phosphorylation regulates cytokinesis. *Sci Signal* 2010; 3: ra2.
43. Nahser PJ Jr., Brown RE, Oskarsson H, et al. Maximal coronary flow reserve and metabolic coronary vasodilation in patients with diabetes mellitus. *Circulation* 1995; 91: 635–640.
44. Levelt E, Rodgers CT, Clarke WT, et al. Cardiac energetics, oxygenation, and perfusion during increased workload in patients with type 2 diabetes mellitus. *Eur Heart J* 2016; 37: 3461–3469.
45. Sorensen MH, Bojer AS, Broadbent DA, et al. Cardiac perfusion, structure, and function in type 2 diabetes mellitus with and without diabetic complications. *Eur Heart J Cardiovasc Imaging* 2020; 21: 887–895.
46. Kofflard MJ, Michels M, Krams R, et al. Coronary flow reserve in hypertrophic cardiomyopathy: relation with microvascular dysfunction and pathophysiological characteristics. *Neth Heart J* 2007; 15: 209–215.
47. Camici PG, d’Amati G and Rimoldi O. Coronary microvascular dysfunction: mechanisms and functional assessment. *Nat Rev Cardiol* 2015; 12: 48–62.
48. Taqueti VR and Di Carli MF. Coronary microvascular disease pathogenic mechanisms and therapeutic options: JACC State-of-the-Art Review. *J Am Coll Cardiol* 2018; 72: 2625–2641.
49. Tjoe B, Barsky L, Wei J, et al. Coronary microvascular dysfunction: Considerations for diagnosis and treatment. *Cleve Clin J Med* 2021; 88: 561–571.
50. Hinkel R, Howe A, Renner S, et al. Diabetes mellitus-induced microvascular destabilization in the myocardium. *J Am Coll Cardiol* 2017; 69: 131–143.
51. Torella D, Ellison GM, Torella M, et al. Carbonic anhydrase activation is associated with worsened pathological remodeling in human ischemic diabetic cardiomyopathy. *J Am Heart Assoc* 2014; 3: e000434.

52. Chung AW, Hsiang YN, Matzke LA, et al. Reduced expression of vascular endothelial growth factor paralleled with the increased angiostatin expression resulting from the upregulated activities of matrix metalloproteinase-2 and -9 in human type 2 diabetic arterial vasculature. *Circ Res* 2006; 99: 140–148.
53. Messaoudi S, Milliez P, Samuel JL, et al. Cardiac aldosterone overexpression prevents harmful effects of diabetes in the mouse heart by preserving capillary density. *FASEB J* 2009; 23: 2176–2185.
54. Luo B, Soesanto Y and McClain DA. Protein modification by O-linked GlcNAc reduces angiogenesis by inhibiting Akt activity in endothelial cells. *Arterioscler Thromb Vasc Biol* 2008; 28: 651–657.
55. Ngho GA, Facundo HT, Zafir A, et al. O-GlcNAc signaling in the cardiovascular system. *Circ Res* 2010; 107: 171–185.
56. Hart GW. Three decades of research on O-GlcNAcylation - A major nutrient sensor that regulates signaling, transcription and cellular metabolism. *Front Endocrinol* 2014; 5: 183.
57. Loaeza-Reyes KJ, Zenteno E, Moreno-Rodriguez A, et al. An overview of glycosylation and its impact on cardiovascular health and disease. *Front Mol Biosci* 2021; 8: 751637.
58. Issad T, Al-Mukh H, Bouaboud A, et al. Protein O-GlcNAcylation and the regulation of energy homeostasis: lessons from knock-out mouse models. *J Biomed Sci* 2022; 29: 64.
59. Murata K, Morino K, Ida S, et al. Lack of O-GlcNAcylation enhances exercise-dependent glucose utilization potentially through AMP-activated protein kinase activation in skeletal muscle. *Biochem Biophys Res Commun* 2018; 495: 2098–2104.
60. Shi H, Munk A, Nielsen TS, et al. Skeletal muscle O-GlcNAc transferase is important for muscle energy homeostasis and whole-body insulin sensitivity. *Mol Metab* 2018; 11: 160–177.
61. Jo S, Pritchard S, Wong A, et al. Pancreatic beta-cell hyper-O-GlcNAcylation leads to impaired glucose homeostasis *in vivo*. *Front Endocrinol (Lausanne)* 2022; 13: 1040014.
62. Keembiyehetty C, Love DC, Harwood KR, et al. Conditional knock-out reveals a requirement for O-linked N-Acetylglucosaminase (O-GlcNAcase) in metabolic homeostasis. *J Biol Chem* 2015; 290: 7097–7113.
63. Sinha A, Rahman H, Webb A, et al. Untangling the pathophysiologic link between coronary microvascular dysfunction and heart failure with preserved ejection fraction. *Eur Heart J* 2021; 42: 4431–4441.
64. Tona F, Montisci R, Iop L, et al. Role of coronary microvascular dysfunction in heart failure with preserved ejection fraction. *Rev Cardiovasc Med* 2021; 22: 97–104.
65. Hu Y, Belke D, Suarez J, et al. Adenovirus-mediated overexpression of O-GlcNAcase improves contractile function in the diabetic heart. *Circ Res* 2005; 96: 1006–1013.
66. Angiogenesis Protocols. Third Edition. *Anticancer Res* 2016; 36: 4370.
67. Arnaoutova I, George J, Kleinman HK, et al. The endothelial cell tube formation assay on basement membrane turns 20: state of the science and the art. *Angiogenesis* 2009; 12: 267–274.
68. Prisco AR, Bukowy JD, Hoffmann BR, et al. Automated quantification reveals hyperglycemia inhibits endothelial angiogenic function. *PLoS One* 2014; 9: e94599.
69. Chen D, Wang Y, Liu M, et al. Visfatin promotes angiogenesis of RF/6A cells through upregulation of VEGF/VEGFR-2 under high-glucose conditions. *Exp Ther Med* 2021; 21: 389.
70. Wang JJ, Wu KF and Wang DD. A novel regulatory network of linc00174/miR-150-5p/VEGFA modulates pathological angiogenesis in diabetic retinopathy. *Can J Physiol Pharmacol* 2021; 99: 1175–1183.
71. Zibrova D, Vandermoere F, Goransson O, et al. GFAT1 phosphorylation by AMPK promotes VEGF-induced angiogenesis. *Biochem J* 2017; 474: 983–1001.
72. Yoon YS, Uchida S, Masuo O, et al. Progressive attenuation of myocardial vascular endothelial growth factor expression is a seminal event in diabetic cardiomyopathy: restoration of microvascular homeostasis and recovery of cardiac function in diabetic cardiomyopathy after replenishment of local vascular endothelial growth factor. *Circulation* 2005; 111: 2073–2085.
73. Kageyama S, Yokoo H, Tomita K, et al. High glucose-induced apoptosis in human coronary artery endothelial cells involves up-regulation of death receptors. *Cardiovasc Diabetol* 2011; 10: 73.
74. Beishline K and Azizkhan-Clifford J. Sp1 and the 'hallmarks of cancer'. *FEBS J* 2015; 282: 224–258.
75. Radhakrishnan R and Kowluru RA. Long noncoding RNA MALAT1 and regulation of the antioxidant defense system in diabetic retinopathy. *Diabetes* 2021; 70: 227–239.
76. Josko J and Mazurek M. Transcription factors having impact on vascular endothelial growth factor (VEGF) gene expression in angiogenesis. *Med Sci Monit* 2004; 10: RA89–98.
77. Corre I, Paris F and Huot J. The p38 pathway, a major pleiotropic cascade that transduces stress and metastatic signals in endothelial cells. *Oncotarget* 2017; 8: 55684–55714.
78. Xue M, Shi Y, Pang A, et al. Corin plays a protective role via upregulating MAPK and downregulating eNOS in diabetic nephropathy endothelial dysfunction. *FASEB J* 2020; 34: 95–106.
79. Huang A, Yang YM, Yan C, et al. Altered MAPK signaling in progressive deterioration of endothelial function in diabetic mice. *Diabetes* 2012; 61: 3181–3188.
80. Pernow J, Kiss A, Tratsiakovich Y, et al. Tissue-specific up-regulation of arginase I and II induced by p38 MAPK mediates endothelial dysfunction in type 1 diabetes mellitus. *Br J Pharmacol* 2015; 172: 4684–4698.
81. Lu Q, Zhang X, Liang T, et al. O-GlcNAcylation: an important post-translational modification and a potential therapeutic target for cancer therapy. *Mol Med* 2022; 28: 115.